Materials Physics and Mechanics 46 (2020) 115-121 Received: October 15, 2020

SIMULATION OF INVERSE HALL-PETCH RELATION IN NANOCRYSTALLINE CERAMICS BY DISCRETE DISLOCATION DYNAMICS METHOD

S.V. Bobylev*

Institute of Problems of Mechanical Engineering, Russian Academy of Sciences, Bolshoj 61, Vas. Ostrov, St. Petersburg 199178, Russia

Peter the Great St. Petersburg Polytechnic University, Politechnicheskaya 29, St. Petersburg 195251, Russia

*e-mail: bobylev.s@gmail.com

Abstract. A theoretical model of plastic deformation of nanocrystalline ceramics in the region of small grain sizes is proposed. In the framework of the model, deformation is described as the combined action of grain boundary sliding and emission of lattice dislocations from triple junctions of grain boundaries. Using the method of discrete dislocation dynamics we obtained an inverse Hall-Petch relation, which qualitatively coincides with the experimentally measured dependences of microhardness in nanocrystalline ceramics with extremely small grain sizes.

Keywords: discrete dislocation dynamics, inverse Hall-Petch relation, ceramics, yield stress, hardness

1. Introduction

The high strength and hardness of nanocrystalline ceramics make them good candidates for use in various industries, including electronics, optics, and power engineering [1-6]. Usually, the microhardness of ceramics obeys the Hall-Petch relation, which predicts a linear dependence between microhardness and the inverse square root of the grain size [7-9]. At the same time, several research groups [10-16] have demonstrated an inverse Hall-Petch relation (i.e., a decrease in microhardness with a decrease in grain size) in various nanocrystalline ceramics at grain sizes below a certain critical value. At the same time, the authors of Refs. [17,18] recently succeeded in synthesizing superstrong nanocrystalline $MgAl_2O4$ and $ZnAl_2O_4$ ceramics, which demonstrated the direct Hall-Petch relation down to grain sizes of 7 and 10 nm, respectively. The reason for these contradictory results is not yet clear, and for their explanation, it is necessary to understand the processes of plastic deformation occurring in nanoceramics.

Molecular dynamics simulations [16,19,20] and experiments [16,21] have demonstrated the important role of deformation processes associated with grain boundaries (for example, grain boundary sliding and grain rotations), as well as processes of intragranular dislocation plasticity and formation of shear bands. In these works, a transition was observed from predominantly intragrain plasticity to grain boundary mediated deformation processes with a decrease in the grain size. The processes of plastic deformation in nanocrystalline ceramics, as well as the direct and inverse Hall-Petch relation for such materials, were also studied in theoretical works [12,22,23]. Authors of Refs. [12,22] utilized phenomenological composite models, which do not take into account any physical mechanisms of plastic deformation. In a

http://dx.doi.org/10.11585/MPM.4612020_11

recent theoretical work [23], the transition from intragranular dislocation plasticity to sliding along grain boundaries was considered. As a result, the authors of [23] were able to explain the existence of both direct and inverse Hall-Petch dependences in nanocrystalline ceramics with very small grain sizes. At the same time, the assumptions of the model [23] about thermally activated sliding along grain boundaries, predicting a significant dependence of the microhardness on the strain rate, could not explain the observed [15] weak dependence of the microhardness on the strain rate in nanocrystalline $MgAl_2O_4$ ceramics.

At present, there is no universal physically substantiated model explaining the presence of the inverse Hall-Petch relation in nanocrystalline ceramics, together with other experimental data. In this work, we propose a model of plastic deformation of nanocrystalline ceramics realized via grain boundary sliding in combination with the emission of lattice dislocations from the regions of grain boundaries adjacent to triple junctions. To calculate the yield stress within the framework of this model and explain the inverse Hall-Petch relation for nanocrystalline ceramics, we will use the method of discrete dislocation dynamics, which is briefly described in the next section.

2. Discrete dislocation dynamics method: brief description

Discrete dislocation dynamics (DDD) is a common method for describing the motion of dislocations, which makes it possible to clearly track the positions of individual dislocations and calculate the accumulation of plastic deformation in a material. In this work, we propose a simple two-dimensional model, which in the future can be extended to the three-dimensional case in a fairly obvious, albeit time-consuming way. In the framework of two-dimensional DDD, edge dislocations are modeled as point sources of deformation, characterized by the Burgers vector **b**. The dislocations are assumed to be straight and infinitely long in the direction perpendicular to the model plane. The force **F** acting on a dislocation is given by the well-known expression (the Peach-Koehler force [24]):

$$\mathbf{F} = (\boldsymbol{\sigma} \cdot \mathbf{b}) \times \boldsymbol{\xi}, \tag{1}$$

where $\boldsymbol{\sigma}$ is the tensor of elastic stresses created by all dislocations and the externally applied load, and $\boldsymbol{\xi}$ is the unit vector specifying the direction of the dislocation line. The dislocation velocity **v** can then be determined using the law of motion [25]:

$$\mathbf{v} = \mathbf{M} \cdot \mathbf{F}, \tag{2}$$

where **M** is the mobility tensor. In the simple case considered here, when dislocations are able to move only in one slip plane (which is typical for fcc structures), the tensor **M** is given by the expression:

$$\mathbf{M} = m_g (\mathbf{I} - \mathbf{n} \otimes \mathbf{n}), \tag{3}$$

where m_g is dislocation mobility constant, **I** is the identity matrix, **n** is the vector normal to the slip plane of the dislocation. The time dependence of the dislocation position $r_i(t)$ in its slip plane is found as a result of the iterative process:

$$r_i(t + \Delta t) = r_i(t) + v_i(t)\Delta t, \tag{4}$$

where $v_i(t)$ is the dislocation velocity **v** projection on the glide direction and Δt is the time step. Tracking all dislocation positions we can easily calculate the total plastic strain accumulated in the material at any given time.

Within the framework of the DDD approach, two main mechanisms are usually introduced: (1) nucleation of dislocations and (2) annihilation of dislocations. In the two-dimensional approach, the nucleation of dislocations is described by randomly placing point dislocation sources of the Frank-Read type. When triggered, such a source generates a pair (dipole) of dislocations of opposite signs, equidistant from the source and spaced from each other at a certain (specified) distance l_s. Nucleation occurs when the effective shear stress at

the source exceeds the specified critical value τ_s (source power). The distance l_s is, in fact, the equilibrium distance between two dislocations under the action of shear stress τ_s, and these quantities are related to each other by the known expression:

$$\tau_s = \frac{Gb}{2\pi(1-\nu)}\frac{1}{l_s}, \tag{5}$$

where G is the shear modulus and ν is Poisson's ratio. Annihilation of dislocations is implemented by removing any pair of dislocations of opposite sign that approach each other at a given (small) distance.

3. Simulation of grain boundary sliding and emission of dislocations from triple junctions of grain boundaries

Commonly the method described above is used to model dislocation plasticity, which is realized via glide of lattice dislocations. However, it is possible to use this method to describe the mechanism of grain boundary sliding. This mechanism is represented (see, for example, [26]), similarly to lattice slip, as the nucleation and slip of grain boundary dislocations along the grain boundary planes. Within the framework of DDD, grain-boundary dislocations are similar to lattice dislocations (except for the magnitude of the Burgers vector).

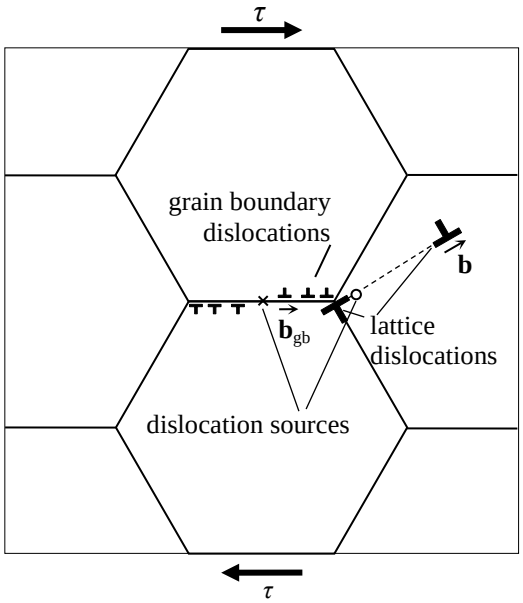

Fig. 1. A model of grain boundary sliding and emission of lattice dislocations from grain boundary triple junctions

A schematic depiction of the grain boundary deformation model is shown in Fig. 1. Consider a fragment of a nanocrystalline structure under the action of external shear stress. The material is assumed to be elastically isotropic and consists of identical hexagonal grains of size d. To simulate grain boundary sliding, we will place the source of grain boundary dislocations on one of the grain boundaries. Since the Burgers vector of grain-boundary dislocations is much smaller than the lattice one, such a source is activated at lower applied stress as compared to the sources of lattice dislocations. Therefore, grain boundary sliding is at first carried out relatively easily until the emitted dislocations begin to accumulate on some obstacle. The main and most important obstacle to the movement of dislocations is the triple junctions of grain boundaries. Their role is especially important in nanocrystalline structures due to the small grain size. In this work, we will not consider the mechanisms of overcoming

barriers by dislocations, i.e., the transfer of plastic shear through a triple junction to neighboring grain boundaries. Consequently, under the action of the applied voltage, the source will successively emit dipoles of grain-boundary dislocations (see Fig. 1), characterized by the Burger's vector, until a sufficient amount of them is accumulated to "lock" the source. Emission and sliding of grain boundary dislocations cause plastic shear along the grain boundary.

As a result of the source's operation, a double pile-up of grain-boundary dislocations is formed at the grain boundary, pressed against the triple junctions. As is known from the theory of dislocations [24], such pile-up is a stress concentrator and the area of the triple junctions are characterized by increased elastic stresses. Consequently, triple junctions can act as sources of heterogeneous nucleation of dislocations, which is regularly observed in molecular dynamics simulations [27,28]. In this work, we will also consider triple junctions as sources of lattice dislocations, activated in the stress field of grain-boundary dislocations pile-ups.

Within the framework of the DDD approach, the process of emission of lattice dislocations from triple joints is simulated by the following method. Near the triple junction where grain-boundary dislocations are accumulated, at a given short distance we place a virtual source of lattice dislocations (see Fig. 1). It is a virtual source in the sense that there is actually no actual Frank-Read source at this point. In reality, a lattice dislocation is emitted as a result of the splitting of the head grain-boundary dislocation of the pile-up. However, such a process is inconvenient to describe within the framework of the DDD formalism. Thus we place an ordinary dislocation source in the vicinity of the triple junction. In this case, the length, and, consequently, the power of the source (see formula (5)), will be determined by the distance to the nearest grain boundary from the dislocation source. The only difference between this source and the standard Frank-Read source is that we do not set a fixed sliding plane for it, but we check it for operation in all possible sliding planes that exist in the material being modeled. As a result of the activation of this source, one of the dislocations remains near the triple junction, and the second goes into the grain body. The dislocation remaining in the triple junction effectively "locks" the source, so the triple junction can emit only one dislocation.

Summing up, the modeled process in this work is presented as follows (Fig. 1). The applied stress activates the source of grain boundary dislocations (marked as $\times$) in the center of one of the grain boundaries, causing the intergranular slip. Grain-boundary dislocations accumulate at the triple junction, which leads to stress concentration in the vicinity of the triple junction. This, in turn, can lead (if the stress is high enough) to the activation of the source of lattice dislocations ($\times$) and the nucleation of one lattice dislocation near the triple junction, and the emission of another lattice dislocation into the grain body.

4. Results and discussion

Following the approach outlined in the previous paragraphs, we simulated plastic deformation in a nanocrystalline material using the example of $MgAl_2O_4$ ceramic bulk material characterized by the following value of parameters. For this, we used the model system shown in Fig. 1 and subjected to shear stress τ. We placed the source of grain-boundary dislocations exactly in the center of the grain boundary and set the distance $l_s = 2$ nm, the Burgers vector of lattice dislocations equal to $b = 0.3$ nm [23], and grain-boundary dislocations – $b_{gb} = b/10$. The virtual source of lattice dislocations was placed at a distance of 2 nm from the triple junction exactly on the grain boundary line. We defined possible lattice slip systems as follows. We assumed that a grain has six possible slip planes defined by an angle $\varphi = n\pi/3$ (where n is an integer) relative to a randomly specified orientation

$0 \le \theta < \pi/3$ of the grain itself (relative to the reference coordinate system). Since in this work we are interested in the inverse Hall-Petch dependence, we simulated a material with very small grain size, in which there are no sources of lattice dislocations in the volume of grains (except for virtual sources near triple junctions).

Figure 2 shows the calculated dependences of the plastic shear strain on the applied stress τ for different grain sizes. The dependences clearly show a strain jump corresponding to the moment of emission of a lattice dislocation from a triple junction. Translating shear into tensile deformation, we also calculated the dependence of the conventional tensile yield stress $\sigma_{0,2}$ on the grain size (Fig. 3). Figure 3 clearly demonstrates the inverse Hall-Petch dependence in the range of grain sizes from 10 to 50 nm – an increase in the yield stress with an increase in the grain size.

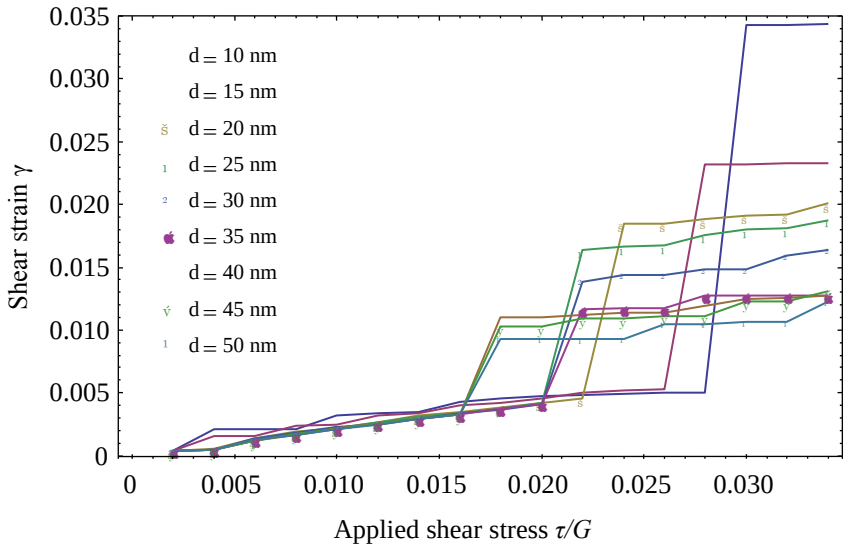

Fig. 2. Shear strain γ dependence on applied shear stress τ for various grain sizes of nanocrystalline $MgAl_2O_4$ ceramic

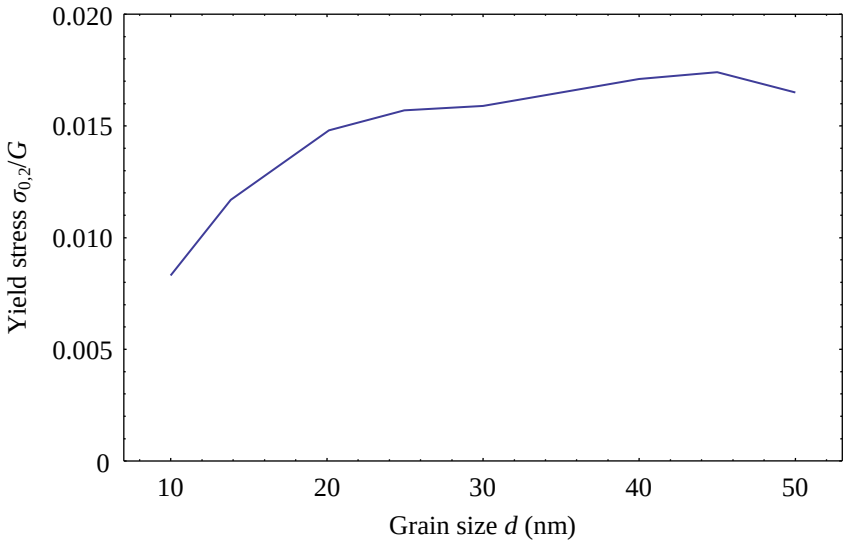

Fig. 3. Yield stress $\sigma_{0.2}$ dependence on the grain size d of nanocrystalline $MgAl_2O_4$ ceramic

It should be noted that the simplified nature of the model does not allow obtaining realistic absolute values of the yield stress that coincide with the experimental data. While our simulations estimate yield stress at the level of $0.01–0.02G$ (which for $MgAl_2O_4$ ceramic with

$G \approx 100$ GPa gives ~1–2 GPa), the experimental data on microhardness measurements in nanocrystalline ceramics [10-16] reports typical values of $H_V = 20 - 30$ GPa, which translates (using standard phenomenological relation $H_V = 3\sigma_{0.2}$) to yield stress of the order of 6–10 GPa. So our data significantly underestimate yield stress (microhardness). The discrepancy in absolute values of calculated and measured yield stress is most likely attributed to the lack of certain deformation mechanisms specific to $MgAl_2O_4$ ceramic in our model. For example, it is possible that the transfer of plastic shear through a triple junction to neighboring grain boundaries, grain rotation, and GB amorphization might play a significant role. Also, choice of model parameters (such as dislocation mobility and source strength) might be improved.

At the same time, the qualitative nature of the dependences coincides with the experimental data on microhardness measurements in nanocrystalline ceramics [10-16]. Further research is planned to improve the proposed model.

5. Conclusion

Thus, in this work, we have proposed a theoretical model of deformation of nanocrystalline ceramics, which describes the inverse Hall-Petch relation in the region of small grain sizes. The model was verified by the method of discrete dislocation dynamics. The results of the model showed a qualitative agreement with the experimental data. We can conclude that grain boundary sliding combined with intragrain plasticity seems to reasonably explain the experimental observations.

Acknowledgements. *This work was supported by the Russian Science Foundation, grant 18-19-00255.*

References

[1] Mayo MJ, Hague DC, Chen DJ. Processing nanocrystalline ceramics for applications in superplasticity. *Mater. Sci. Eng. A.* 1993;166(1-2): 145-159.

[2] Mayo MJ. Processing of nanocrystalline ceramics from ultrafine particles. *Intern. Mater. Rev.* 1996;41(3): 85-115.

[3] Kleinlogel C, Gauckler LJ. Sintering of Nanocrystalline CeO_2 Ceramics. *Adv. Mater.* 2001;13(14): 1081-1085.

[4] Kalita SJ, Bhardwaj A, Bhatt HA. Nanocrystalline Calcium Phosphate Ceramics in Biomedical Engineering. *Mater. Sci. Eng. C.* 2007;27(3): 441-449.

[5] Cheng FY, Shen JA, Peng B, Pan YD, Tao ZL, Chen J. Rapid room-temperature synthesis of nanocrystalline spinels as oxygen reduction and evolution electrocatalysts. *Nature Chemistry*. 2011;3(1): 79-84.

[6] Mudinepalli VR, Feng L, Lin WC, Murty BS. Effect of grain size on dielectric and ferroelectric properties of nanostructured $Ba_{0.8}Sr_{0.2}TiO_3$ ceramics. *J. Adv. Ceramics.* 2015;4: 46-53.

[7] Wollmershauser JA, Feigelson BN, Gorzkowski EP, Ellis CT, Goswami R, Qadri SB, Tischler JG, Kub FJ, Everett RK. An extended hardness limit in bulk nanoceramics. *Acta Mater.* 2014;69: 9-16.

[8] Sokol M, Halabi M, Kalabukhov S, Frage N. Nano-structured $MgAl_2O_4$ spinel consolidated by high pressure spark plasma sintering (HPSPS). *J. Europ. Ceram. Soc.* 2017;37(2): 755-762.

[9] Sokol M, Kalabukhov S, Shneck R, Zaretsky E, Frage N. Effect of grain size on the static and dynamic mechanical properties of magnesium aluminate spinel ($MgAl_2O_4$). *J. Europ. Ceram. Soc.* 2017;37(10): 3417-3424.

[10] Wang H, Sharma A, Kvit A, Wei Q. Mechanical properties of nanocrystalline and epitaxial TiN films on (100) silicon. *J. Mater. Res.* 2001;16(9): 2733-2738.
[11] Wang Y, Zhang J, Zhao Y. Strength weakening by nanocrystals in ceramic materials. *Nano Lett.* 2007;7(10): 3196-3199.
[12] Ehre D, Chaim R. Abnormal Hall-Petch Behavior in Nanocrystalline MgO Ceramic. *J. Mater. Sci.* 2008;43(18): 6139-6143.
[13] Qi ZB, Sun P, Zhu FP, Wang ZC, Peng DL, Wu CH. The inverse Hall–Petch effect in nanocrystalline ZrN coatings. *Surf. Coat. Tech.* 2011;205(12): 3692-3697.
[14] Sokol M, Halabi M, Mordekovitz Y, Kalabukhov S, Hayun S, Frage N. An inverse Hall-Petch relation in nanocrystalline $MgAl_2O_4$ spinel consolidated by high pressure spark plasma sintering (HPSPS). *Scripta Mater.* 2017;139: 159-161.
[15] Ryou H, Drazin JW, Wahl KJ, Qadri SB, Gorzkowski EP, Feigelson BN, Wollmershauser JA. Below the hall–petch limit in nanocrystalline ceramics. *ACS Nano***.** 2018;12(4): 3083-3094.
[16] Guo D, Song S, Luo R, Goddard III WA, Chen M, Reddy KM, An Q. Grain Boundary Sliding and Amorphization are Responsible for the Reverse Hall-Petch Relation in Superhard Nanocrystalline Boron Carbide. *Phys. Rev. Lett.* 2018;121(14): 145504.
[17] Muche DNF, Drazin JW, Mardinly J, Dey S, Castro RHR. Colossal grain boundary strengthening in ultrafine nanocrystalline oxides. *Mater. Lett.* 2017;186: 298-300.
[18] Yang C, Thron A, Castro RHR. Grain boundary strengthening in nanocrystalline zinc aluminate. *J. Amer. Cer. Soc.* 2019;102(11): 6904-6912.
[19] Szlufarska I, Nakano A, Vashishta P. A crossover in the mechanical response of nanocrystalline ceramics. *Science.* 2005;309(5736): 911-914.
[20] Feng Q, Song X, Liu X, Liang S, Wang H, Nie Z. Compression deformation of WC: atomistic description of hard ceramic material. *Nanotechnology.* 2017;28(47): 475709.
[21] Ratzker B, Wagner A, Sokol M, Meshi L, Kalabukhova S, Frage N. Deformation in nanocrystalline ceramics: A microstructural study of $MgAl_2O_4$. *Acta Mater.* 2020;183: 137-144.
[22] Jiang B, Weng GJ. A theory of compressive yield strength of nano-grained ceramics. *Int. J. Plasticity.* 2004;20(11): 2007-2026.
[23] Sheinerman AG, Castro RHR, Gutkin MY. A model for direct and inverse Hall- Petch relation for nanocrystalline ceramics. *Mater. Lett.* 2020;260: 126886.
[24] Hirth JP, Lothe J. *Theory of dislocations.* New York: Wiley; 1982.
[25] Quek SS, Chooi ZH, Wu Z, Zhang YW, Srolovitz DJ. The inverse hall–petch relation in nanocrystalline metals: A discrete dislocation dynamics analysis. *J. Mech. Phys. Sol.* 2016;88: 252-266.
[26] Quek SS, Wu Z, Zhang YW, Srolovitz DJ. Polycrystal deformation in a discrete dislocation dynamics framework. *Acta Mater.* 2014;75: 92-105.
[27] Schiøtz J, Di Tolla FD, Jacobsen KW. Softening of nanocrystalline metals at very small grain sizes. *Nature.* 1998;391: 561-563.
[28] Schiøtz J, Jacobsen KW. A maximum in the strength of nanocrystalline copper. *Science.* 2003;301(5638): 1357-1359.